Thermal analysis and kinetic study of native silks

Ying Liu[2] · Liutao Yang[1,3] · Chunping Ma[1]

Abstract

In this study, X-ray diffraction (XRD), thermogravimetric (TG) analysis and differential scanning calorimetry (DSC) method were used to analyze the main characteristics of native silks, and to analyze the thermal degradation process of this native silks. Three methods were used: XRD to study its structure, TG to study the thermal degradation process and DSC to study the curve of native silks. The thermal decomposition kinetics of native silks was examined within the heating rates of 5–20 °C min^{-1} in nitrogen atmosphere. Different models of kinetic analysis were used to calculate the activation energies using thermogravimetric data of the thermal degradation process. The activation energies got from Kissinger, Flynn–Wall–Ozawa and Šatava–Šesták models were 217.49, 216.09 and 193.61 kJ mol^{-1}, respectively. The values of activation energy indicated that the thermal degradation of native silks was a single reaction mechanism or the combination of multi-reaction mechanisms. TG-FTIR analysis showed that the main pyrolysis products included water, methane, carbon dioxide, ammonia, and so on.

Keywords Native silks · Kinetic analysis · Thermal decomposition · Activation energy · TG-FTIR

Introduction

Biomaterials have received great attentions due to their unique physical, chemical and biological properties [1–7]. Among the natural polymers, natural silk has been widely used in various textiles but also in consumer staples such as pharmaceuticals, electronic products and household products. Silk is a natural fiber spun by the domestic silkworm, which is a proteinaceous fiber consists of two filaments of protein, fibroin, with high crystallinity and strong preferred orientation. This material is nontoxic and harmless and has good biocompatibility. Therefore, silk fibroin is attractive as a biomaterial. Recently, *Bombyx mori* larval silkworms were fed with single-walled carbon nanotubes and grapheme [8], and the result showed that parts of the carbon nanomaterials were integrated into the silk fibers, whereas the others went into the feces of silkworms.

When heated, the native silk suffers decomposition. Thermal degradation and stability are important aspects from both scientific and industrial fields. The degradation is a complicated process; but in practical application process, it may be adequate to consider only the overall characteristics of the thermal degradation process with some simplified mechanism. Thermal processing has been widely used to evaluate the properties of the textiles and the silk-based materials [9–11].

Thermal analysis is a group of techniques for the rapid assessment of thermal stability, decomposition temperature, absorbed water content, crystal water content, and the thermal degradation dynamics. Thermogravimetric (TG) analysis and differential scanning calorimetry (DSC) method have been used as a prevalent technique to evaluate the thermal stability and degradation of polymers. The assessment of thermal stability and degradation dynamics of native silks is very important in practical applications. For the kinetic analysis, non-isothermal procedure is basically the first choice. And for this aim, many models, such as Kissinger, Šatava–Šesták, Doyle and Coast-

✉ Liutao Yang
215724523@qq.com

1 College of Materials and Metallurgical Engineering, Guizhou Institute of Technology, Guiyang 550003, Guizhou, China

2 College of Chemical Engineering, Guizhou Institute of Technology, Guiyang 550003, Guizhou, China

3 Key Laboratory of Light Metal Materials Processing of Guizhou Province, Guizhou Institute of Technology, Guiyang 550003, Guizhou, China

Redfern, were used to calculate the dynamic parameters based on the Arrhenius equation [12–18].

There have been some reports of the degradation cases of raw or processed silks from many sources using different thermal analysis methods [19, 20]. Dewatering and pyrolysis were usually deemed as the two main stages related to the decomposition mechanism of native silks. The distinctive microstructure of native silk and its multiple phase transformation in the process of heating give an excellent approach to explain the structure–processing–performance relationship. The achievements in the field can increase the knowledge of polymer science, especially the natural polymers. Differences of four silks from African wild silkmoths were studied regarding their thermal degradation behaviors and mechanical performances [21]. The result showed that the differences of four African silks in their mechanical and thermal degradation properties were related to their chemical structure and component. Silk/poly(lactic acid) biocomposites were prepared by using melting compound methods, and the effect of silk protein on the thermal and mechanical performances of the PLA matrix was investigated [22]. The results shown that the stiffness of the PLA matrix incorporated with silk protein at higher temperature was remarkable increased, and the dimension stability was also enhanced, but the thermal stability decreased. Three kinds of wild silks from India were comparatively studied with Chinese mulberry (*Bombyx mori*) silkworm fibers. The results showed that wild silks had higher thermal stabilities and alterable degradation profiles [23].

However, the thermal decomposition kinetics of native silks has not been reported. Thermal analysis study of materials helps to understand the kinetic and the mechanism of their thermal decomposition. Practically, thermokinetic studies can provide valuable information on thermal stability and shelf life of these materials to store at different conditions. Specifically, thermal analysis study of polymeric materials helps to evaluate their exothermic decomposition on the possible risks in their transport, processing and storage. The main purpose of this study was to survey the thermal processing by TG and DSC to calculate the kinetic parameters during the thermal degradation of native silks. In this study, three methods were used: XRD to study its structure, TG to study the thermal degradation process, and DSC to study the curve of native silks. Degradation processes were made in TG with four different heating rates. These data were used to analyze the thermal degradation kinetics using different isoconversional methods like Kissinger, Flynn–Wall–Ozawa, and Šatava–Šesták models, which used to evaluate the activation energy of native silks.

Experimental

Materials

The native silkworm silks used in this study were purchased from Guiyang Jincheng CO., Ltd. (Guizhou, China). The dried samples were ground and sieved using a sieve of 0.15 mm in order to get uniform particles for TG/DSC/TG-FTIR measurements. The native silk samples were kept in airtight packages.

X-ray diffraction

The X-ray diffraction pattern was measured using a diffractometer (Siemens D5000) instrument, which was operated at 40 kV and 40 mA, and 2θ range from 5° to 72° with a step size or sampling interval of 0.02°. From the XRD patterns, the interplanar spacings (d) were calculated by Bragg's equation. In order to get the crystallization fraction of native silk sample, the software MDI Jade 5.0 was used.

TG/DSC analysis

A thermal analyzer (STA-625, Reometric Scientific) was used for obtaining TG curves. The thermal analyses were carried out in alumina crucibles under dry argon atmosphere with a flow rate of 10 mL min^{-1}. The starting temperature was 35 °C. The rates of heating were 5, 10, 15, 20 °C min^{-1}, respectively. Each silk sample was about 5 mg.

DSC curve was done using a TA Instruments DSC Q2000 (DE, USA) with a scanning rate of 10 °C min^{-1} under dry argon atmosphere with a flow rate of 50 mL min^{-1}.

TG-FTIR test

Thermogravimetry-Fourier transform infrared spectroscopy (TG-FTIR) analysis was obtained by TG 209F3/Tensor 27 (Netzsch/Bruker), heating under N$_2$ from room temperature to 600 °C with a heating rate of 20 °C min^{-1}.

Results and discussion

Theoretical background

The thermal degradation of native silks is a complex process, because many reactions are involved. The comprehensive dynamic analysis of the complicated process is usually impracticable. However, other types of mean

kinetic description are still feasible. In this research, Kissinger [24], Flynn–Wall–Ozawa [25, 26], and Šatava–Šesták [27, 28] models were used to investigate the thermal degradation process of native silks.

The structural analysis of the native silks

The XRD pattern of native silks is shown in Fig. 1. There was a main peak at about 20.8° and a shoulder at about 24.4°, and a broad maximum peak was observed for the sample which was indicative of a disordered structure of native silks. This pattern was quite similar to the previous results [29]. This is an explicit indication of the existence of two preferential intermolecular interactions in the lateral packing of the backbones. Based on the Bragg's equation, the distances (*d*) were 0.43 and 0.36 nm, respectively.

The structure of the native silks primarily is amorphous. Meanwhile, due to the long and flexible molecular chains hinder further crystallization, only a spot of crystalline structure exist [29]. The crystalline region has a high degree of periodicity with simple repeating parts broken by complicated sections with amino acids containing bulky branched chains. The crystalline parts are composed of *β*-sheets; meanwhile, amorphous parts comprise amino acids which do not partake in *β*-sheet configuration. The coexistence of amorphous parts makes the peak wide.

Thermal degradation

Thermal degradation is a very important part of thermal procedure. Thermogravimetric analysis is a very common method used for research of the thermal degradation process. The thermogravimetric curves of native silks were measured at different heating rates for the research of thermal degradation process with different non-isothermal techniques. Figure 2 shows the thermogravimetric curves of native silks at different heating rate, respectively. These curves present three primary mass loss parts. The first part is the desiccation which starts instantly when the temperature just rises and ends at about 120 °C. The percentage of mass loss in this part is related with the water content of
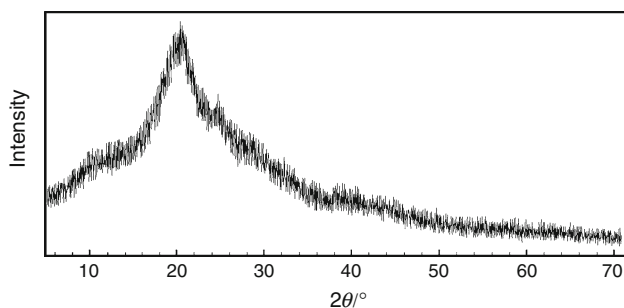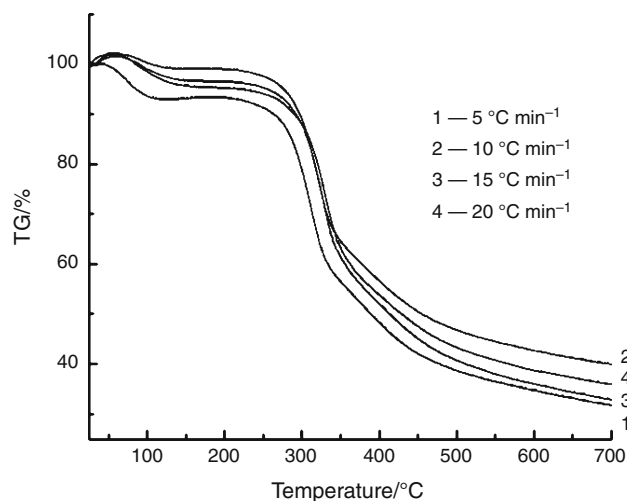

Fig. 2 The thermogravimetric curves of native silks at different heating rates

native silks. The second part is the main degradation stage, which finishes at around 450 °C. Pyrolysis of native silks has been described to give water, carbon dioxide, ammonia and so on [30]. Thermal decomposition has usually been regarded as the important process associated with the degradation mechanisms of native silks. The last step ends with the formation of carbon black at around 700 °C. The most important degradation process of native silks was made in ΔT (the full width at half maximum of DTG curve) = 50, 55, 66, and 70 °C at the heating rates of 5, 10, 15 and 20 °C min^{-1}, respectively.

The dehydration process is generally not deemed to affect the thermal decomposition of native silks, because all water will evaporate before the decomposition of the sample in the open system. Even though the form of the thermogravimetric curves does not change, the starting temperature of decomposition is the same, and the peak temperature increases with the increasing heating rate. This phenomenon is probably ascribed to heat transfer problem between the native silks and equipment [31], and the reason may also be that the fast heating rate leads the native silks to the given temperature rapidly as a result of increased thermal lag [32, 33]. These curves were used for the calculation of dynamics parameters including activation energy and lnA.

Kinetics of thermal degradation analysis

In order to get the dynamics parameters and the most probable mechanism of the thermal degradation process, the thermogravimetric curves at different heating rates were dealt with using three kinetic models.

Fig. 1 XRD pattern of the native silks

Kissinger model

The Kissinger model was used to analyze the thermogravimetric curves of native silks. Figure 3 depicts the fitted curve of $\ln(\beta/T_m^2)$ versus $1000/T_m$ where slopes give $-E/R$, and the correlation coefficient (R^2) is 0.9930. Thus, the Kissinger model can be availably applied in native silks. The Kissinger model can be used to roughly calculate the activation energy of the thermal degradation using the peak value of thermogravimetric curves. Activation energy and $\ln A$ obtained from the slope were 217.49 kJ mol^{-1} and 36.80 min^{-1}, respectively. In general, the activation energy value is in the maximum degradation rate or in the largest heat absorption [34].

Flynn–Wall–Ozawa model

The Flynn–Wall–Ozawa model was also employed to process the thermogravimetric curves of native silks and calculate the corresponding dynamics parameters. From Fig. 1, the peak temperatures of thermogravimetric curves at different heating rates, T_m, were obtained. Figure 4 illustrates the liner plot of $\lg\beta$ versus $1000/T_m$ where slopes give $-E/R$. The linear correlation coefficient is 0.994, and activation energy is 216.09 kJ mol^{-1}. Thus, the Flynn–Wall–Ozawa model is also effective for native silks.

Šatava–Šesták model

The Šatava–Šesták model was also used to process the thermogravimetric curves of native silks. Mechanism function, $G(\alpha) = -\ln(1-\alpha)$, was ultimately chosen after comparison with the others. Figure 5 depicts the liner plot of $\lg\beta$ versus $1000/T_m$ where slopes give $-0.4567E/R$. The mean correlation coefficient (R^2) of the fitted curves is -0.9935. Activation energy is usually regarded as the
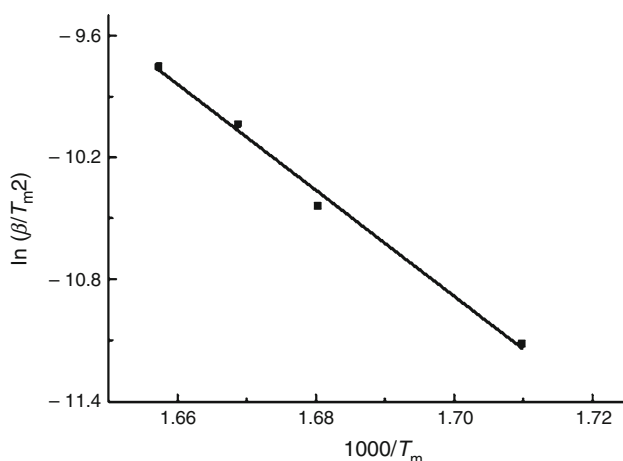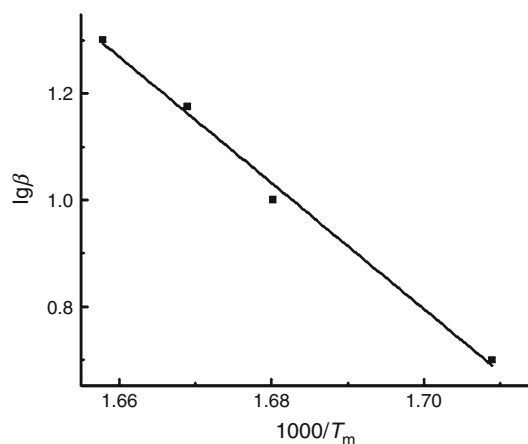

Fig. 3 Kissinger plots of native silks

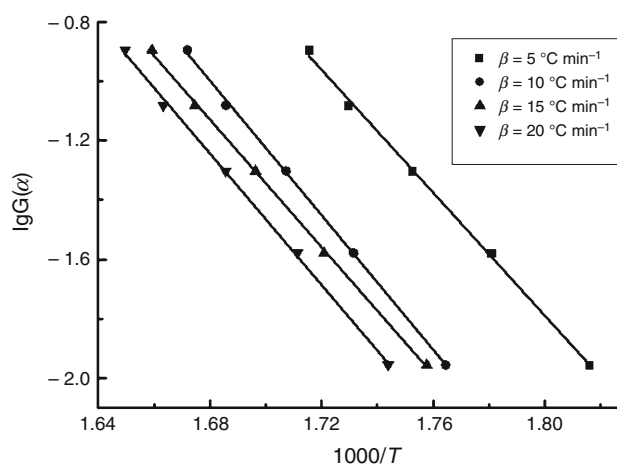**Fig. 4** Flynn–Wall–Ozawa plots of native silks

Fig. 5 Šatava–Šesták plots of native silks

energy barrier to control the bond breaking or bond reapportion step [35]. The activation energies got from the slope ($-0.4567E/R$) are shown in Table 1, and the average value is 193.61 kJ mol^{-1}. It can be seen from Fig. 5 that the fitting curves are approximately parallel, which implies similar activation energies and then indicates the possibility of single reaction mechanism or the combination of multi-reaction mechanisms [36–38].

For the completion of the study and an accurate determination of this behavior, Kissinger, Flynn–Wall–Ozawa, and Šatava–Šesták models were used. The value of

Table 1 The activation energies of native silks using Šatava–Šesták model

β/°C min^{-1}	5	10	15	20
R^2	0.9980	0.9950	0.9990	0.9980
Slope	-10.33	-10.47	-10.71	-11.04
E/kJ mol^{-1}	188.01	190.56	194.92	200.93

activation energy determined by Kissinger model was in good agreement with the value determined by the Flynn–Wall–Ozawa model. The high agreement validated the reliability of calculations and confirmed the predictive power of Kissinger and Flynn–Wall–Ozawa models [39]. Meanwhile, the activation energy values obtained from Šatava–Šesták model was slightly lower than those obtained from the other methods. Based on the three activation energy values, the deviation was 9.64%, which indicated that the results were acceptable. In fact, different kinetic models should be complementary and not competitive [40]. The activation energy alone is insufficient to predict and simulate the entire process of thermal degradation. The satisfactory degradation model should at least include a set of activation energy and pre-exponential factor. However, since the activation energy can provide important information about the transition energy required to initiate a reaction, in this study the range of activation energy can help to investigate the thermal stability of native silks.

DSC studies

The DSC curve was used to study the thermal transformation occurring in the process of heating under an inert atmosphere. The typical DSC curve of native silks in a range of 40–500 °C is presented in Fig. 6. The minor endothermic peak observed below 100 °C seems to be attributable to the evaporation of water in the specimens. The glass transition temperature was about 212 °C, which is in the reported range from 150 to 250 °C [41]. There is a major endothermic peak at 321 °C, which is associated with the degradation of the silk fibroin. After opening the DSC pans, the silks samples were yellow to brown. This change is believed to be due to the interruption of long chains. A large endotherm in a range of 300–400 °C nearly covers all curve transition which represents the
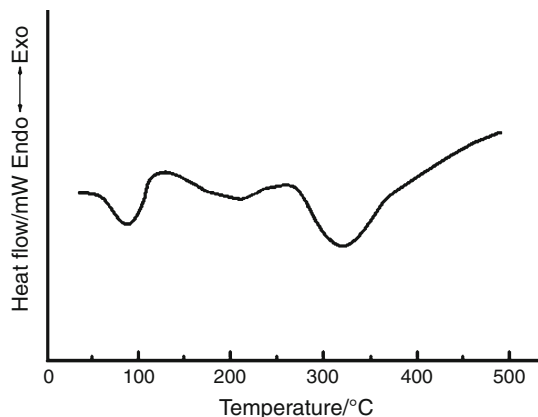

Fig. 6 DSC curve of native silks under heating rate of 10 °C min⁻¹
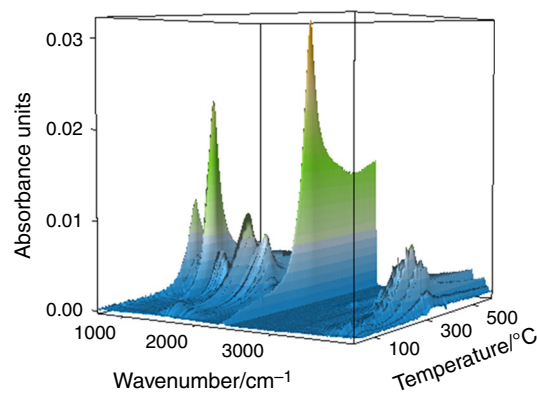

Fig. 7 Three-dimensional FTIR diagram of gaseous products from the pyrolysis of native silks at 20 °C min⁻¹

decomposition of native silks. The result was coincided with those obtained previously from thermogravimetric curves. After opening the DSC pans, the silks samples were carbonized when the temperature was greater than 500 °C. The carbon black directly indicated that the chains of macromolecular had been destroyed.

TG-FTIR analysis

The three-dimensional (3D) FTIR diagram of gaseous products from the pyrolysis of native silks is shown in Fig. 7. By comparison of the standard spectrum of a certain compound, the major products were identified by the appearance of characteristic absorption bands. Carbon dioxide was released quite strongly, causing the absorption at 2349 cm⁻¹ and 667 cm⁻¹. Mainly water vapor was found, which was characterized by peaks at 3736 cm⁻¹. Two narrow bands at about 964 and 927 cm⁻¹ that appeared were the significant peaks of ammonia. The narrow band at 3014 cm⁻¹ indicates the existence of methane. Some other gases could be evolved at the same time, which led to more difficultly find the peak of gas when testing small quantities.

Conclusions

X-ray diffraction, thermogravimetric (TG) analysis and differential scanning calorimetry (DSC) method were applied for studying the main characteristics of native silks. Thermogravimetric curves were used to analyze the thermal degradation kinetics of native silks by non-isothermal process. The Activation energy values of native silks were 217.49, 216.09 and 193.61 kJ mol⁻¹ based on Kissinger, Flynn–Wall–Ozawa, and Šatava–Šesták models, respectively. The results of activation energy show that the thermal decomposition of native silks has a single reaction

mechanism or the combination of multi-reaction mechanisms. The gaseous products from the pyrolysis of native silks were water, carbon dioxide, ammonia, methane, and so on.

References

1. Brown TE, Anseth KS. Spatiotemporal hydrogel biomaterials for regenerative medicine. Chem Soc Rev. 2017;46:6532–52.
2. Wang RM, Johnson TD, He JJ, Rong ZL, Wong M, Nigam V, et al. Humanized mouse model for assessing the human immune response to xenogeneic and allogeneic decellularized biomaterials. Biomaterials. 2017;129:98–110.
3. Liu Y, Yang LT, Ma CP, Zhang YZ. Thermal behavior of sweet potato starch by non-isothermal thermogravimetric analysis. Materials. 2019;12:699.
4. Bose S, Ke D, Sahasrabudhe H, Bandyopadhyay A. Additive manufacturing of biomaterials. Prog Mater Sci. 2018;93:45–111.
5. Zhang GY, Hui HY, Chu PH, Yuan ZB, Chang R, Risteen B, et al. From staple food to flexible substrate to electronics: rice as a biocompatible precursor for flexible electronic components. Chem Mater. 2016;28:8475–9.
6. Prashantha K, Roger F. Multifunctional properties of 3D printed poly (lactic acid)/graphene nanocomposites by fused deposition modeling. J Macromol Sci A. 2017;54:24–9.
7. Wang Q, Wang CY, Zhang MC, Jian MQ, Zhang YY. Feeding single-walled carbon nanotubes or graphene to silkworms for reinforced silk fibers. Nano Lett. 2016;16:6695–700.
8. Wang YX, Tan YB. Long circulating 10-hydroxycamptothecin-loaded nanoparticles fabricated from poly (ethylene glycol)/poly (L-lactic acid) multiblock copolymers. J Macromol Sci A. 2016;53:636–43.
9. Guan J, Wang Y, Mortimer B, Holland C, Shao ZZ, Porter D, et al. Glass transitions in native silk fibres studied by dynamic mechanical thermal analysis. Soft Matter. 2016;12:5926–36.
10. Wang F, Yu HY, Gu ZG, Si L, Liu QC, Hu X. Impact of calcium chloride concentration on structure and thermal property of Thai silk fibroin films. J Therm Anal Calori. 2017;130:851–9.
11. Yazawa K, Ishida K, Masunaga H, Hikima T, Numata K. Influence of water content on the β-sheet formation, thermal stability, water removal, and mechanical properties of silk materials. Biomacromol. 2016;17:1057–66.
12. Yang LT, Liu Y, Wu YJ, Deng LL, Liu W, Ma CP, et al. Thermal degradation kinetics of leather fibers treated with fire-retardant melamine resin. J Therm Anal Calori. 2016;123:413–20.
13. Singh A, Sharma TC, Kishore P. Thermal degradation kinetics and reaction models of 1,3,5-triamino-2,4,6-trinitrobenzene-based plastic-bonded explosives containing fluoropolymer matrices. J Therm Anal Calori. 2017;129:1403–14.
14. Yang LT, Liu Y, Ma CP, Wu YJ, Liu W, Zhang C, et al. Kinetics of non-isothermal decomposition and flame retardancy of goatskin fiber treated with melamine-based flame retardant. Fiber Polym. 2016;17:1018–24.
15. Thakur LS, Varma AK, Mondal P. Analysis of thermal behavior and pyrolytic characteristics of vetiver grass after phytoremediation through thermogravimetric analysis. J Therm Anal Calori. 2018;131:3053–64.
16. Leena K, Soumyamol PB, Baby M, Suraj S, Rajeev R, Mohan DS. Non-isothermal cure and decomposition kinetics of epoxy–imidazole systems. J Therm Anal Calori. 2017;130:1053–61.
17. Ghaemy M, Nasab SMA, Taghavi M, Hassanzadeh M. Study kinetics of thermal decomposition and electrochemical oxidation by using nanocomposite paste of novel poly(amide-ether)s derived from asymmetric diamine. J Macromol Sci A. 2012;49(9):772–83.
18. Wako FM, Reshad AS, Goud VV. Thermal degradation kinetics study and thermal cracking of waste cooking oil for biofuel production. J Therm Anal Calori. 2018;131:2157–65.
19. Kweon HY, Um IC, Park YH. Thermal behavior of regenerated *Antheraea pernyi* silk fibroin film treated with aqueous methanol. Polymer. 2000;20:7361–7.
20. Hu X, Kaplan D, Cebe P. Effect of water on the thermal properties of silk fibroin. Thermochim Acta. 2007;461:137–44.
21. Teshome A, Onyari JM, Raina SK, Kabaru JM, Vollrath F. Mechanical and thermal degradation properties of silk from African wild silkmoths. J Appl Polym Sci. 2013;127:289–97.
22. Zhao YQ, Cheung HY, Lau KT, Xu CL, Zhao DD, Li HL. Silkworm silk/poly (lactic acid) biocomposites: dynamic mechanical, thermal and biodegradable properties. Polym Degrad Stabil. 2010;95:1978–87.
23. Mazzi S, Zulker E, Buchicchio J, Anderson B, Hu X. Comparative thermal analysis of Eri, Mori, Muga, and Tussar silk cocoons and fibroin fibers. J Therm Anal Calori. 2014;116:1337–43.
24. Kissinger HE. Reaction kinetics in differential thermal analysis. Anal Chem. 1957;29:1702–6.
25. Flynn JH, Wall LA. A quick, direct method for the determination of activation energy from thermogravimetric data. J Polym Sci Part B Polym Lett. 1966;4:323–8.
26. Ozawa T. A new method of analyzing thermogravimetric data. Bull Chem Soc Jpn. 1965;38:1881–6.
27. Škvára F, Šesták J. Computer calculation of the mechanism and associated kinetic data using a non-isothermal integral method. J Therm Anal Calorim. 1975;8:477–89.
28. Šatava V. Mechanism and kinetics from non-isothermal TG traces. Thermochim Acta. 1971;2:423–8.
29. Hino T, Tanimoto M, Shimabayashi S. Change in secondary structure of silk fibroin during preparation of its microspheres by spray-drying and exposure to humid atmosphere. J Colloid Interf Sci. 2003;266:68–73.
30. Zhang H, Magoshi J, Becker M, Chen JY, Matsunaga R. Thermal properties of *Bombyx mori* silk fibers. J Appl Polym Sci. 2002;86:1817–20.
31. Garcìa-Pèrez M, Chaala A, Yang J, Roy C. Co-pyrolysis of sugarcane bagasse with petroleum residue. Part I: thermogravimetric analysis. Fuel. 2001;80:1245–58.
32. Jeguirim M, Trouvé G. Pyrolysis characteristics and kinetics of *Arundo donax* using thermogravimetric analysis. Bioresource Technol. 2009;100:4026–31.
33. Vamvuka D, Kakaras E, Kastanaki E, Grammelis P. Pyrolysis characteristics and kinetics of biomass residuals mixtures with lignite. Fuel. 2003;82:1949–60.
34. Huang MX, Zhou CR, Han XW. Investigation of thermal decomposition kinetics of taurine. J Therm Anal Calori. 2013;113:589–93.
35. Rudnik E, Matuschek G, Milanov N, Kettrup A. Thermal stability and degradation of starch derivatives. J Therm Anal Calorim. 2006;85:267–70.

36. Liu XX, Yu L, Xie FW, Li M, Chen L, Li XX. Kinetics and mechanism of thermal decomposition of cornstarches with different amylose/amylopectin ratios. Starch. 2010;62:139–46.

37. Yao F, Wu QL, Lei Y, Guo WH, Xu YJ. Thermal decomposition kinetics of natural fibers: activation energy with dynamic thermogravimetric analysis. Polym Degrad Stabil. 2008;93:90–8.

38. Ravi P, Gore GM, Sikder AK, Tewari SP. Thermal decomposition kinetics of 1-methyl-3,4,5-trinitropyrazole. Thermochim Acta. 2012;528:53–7.

39. Lopez-Velazquez MA, Santes V, Balmaseda J, Torres-Garcia E. Pyrolysis of orange waste: a thermo-kinetic study. J Anal Appl Pyrol. 2013;99:170–7.

40. Brown ME, Maciejewski M, Vyazovkin S, Nomen R, Sempere J, Burnham A, et al. Computational aspects of kinetic analysis: part A: the ICTAC kinetics project-data, methods and results. Thermochim Acta. 2000;355:125–43.

41. Yuan QQ, Yao JR, Huang L, Chen X, Shao ZZ. Correlation between structural and dynamic mechanical transitions of regenerated silk fibroin. Polymer. 2010;51:6278–83.